Titanium dioxide based nanotreatments to inhibit microalgal fouling on building stone surfaces.

Titanium dioxide based nanotreatments to inhibit microalgal fouling on building stone surfaces

Giovanni Battista Goffredo [a]
Stefano Accoroni [b]
Cecilia Totti [b]
Tiziana Romagnoli [b]
Laura Valentini [c]
Placido Munafò [a]

[a] Department of civil and building engineering and architecture, polytechnic university of Marche, 12, via Brecce Bianche, 60131 Ancona, Italy
[b] Department of biomolecular science, biotechnology section, university of Urbino "Carlo Bo", 2, via Arco d'Augusto, 61032 Fano, Italy
[c] Department of life and environmental sciences, polytechnic university of Marche, 12, via Brecce Bianche, 60131 Ancona, Italy
[d] Department of science and engineering of matter and environment and urban planning (SIMAU), polytechnic university of Marche, 12, via Brecce Bianche, 60131 Ancona, Italy
[e] Department of pure and applied sciences, university of Urbino, 13, Piazza della Repubblica, 61029 Urbino, Italy

Highlights

• Stones are materials largely used for building and monuments.

• Algal growth may negatively influence the visual quality of architectural surfaces.

• TiO2-based compounds were tested to assess their effect against algal development.

• Metal nanoparticles (Ag, Cu) were used to increase the biocidal property of TiO2.

• Metallic nanoparticles influenced algal growth but further analyses are needed.

Abstract

Stones are among the most widespread traditional materials used in construction for both structural and ornamental purposes, especially for Cultural Heritage monuments. Stone materials – both natural and man-made – are quite prone to algal colonisation that may cause biodeterioration of building materials by both affecting the aesthetic of their surfaces and compromising their entirety and durability. Nanotechnology has been recently used in both Cultural Heritage and construction industry to improve the preservation of building surfaces and titanium dioxide (TiO2) in its nanometric form is among the most used and promising nanotechnological material.
This study investigated the biocidal ability of photocatalytic TiO2-based nanocompounds (also in combination with Ag and Cu nanoparticles) applied on travertine surfaces by spray-coating in order to limit or inhibit algal fouling. The aesthetic compatibility with stone has been assessed using colorimetry. Algal fouling was simulated by means of an accelerated water run-off test under artificial solar light and weak UV irradiation. Antialgal capability of metallic nanotreatments was evaluated through the combination of different parameters monitored for 9 weeks: human perception of the colour change, reflectance reduction and measurement of area colonised by algae. Nanoproducts had a limited impact on surface colour of the substrate after application making them suitable for restoration. Even though photocatalysis prevented algal fouling only partially, some nanotreatments moderately reduced the bioreceptivity of coated stones – mainly limiting the area colonised by microalgae. Further investigations are necessary, since the conditions used to accelerate algal growth may affect greatly the biocidal efficiency of nanotreatments.

Keywords

Titanium dioxide**,** Photocatalysis**,** Metallic nanoparticles**,** Biocid eAlgal biodeterioration**,** Building stones preservation

1. Introduction

Stones have been used diffusely in architecture since ancient times – especially for structures, claddings and artworks – and like other building materials exposed outdoor may be affected by different sources of decay altering their properties over time, including their appearance. A very wide range of factors may influence the visual quality of architectural stones over time: their own characteristics (mainly surface roughness, porosity and chemical composition) [1], [2], [3], [4], natural weathering, urban pollution, growth of microorganisms, bird droppings, fire damage, salt efflorescence, building defects, conservative treatments (including cleaning) [4], design features [5] and environmental conditions (such as humidity and irradiation) [6].

In this study, we focused on biodeterioration, i.e. the ability of biological activity to deteriorate

building materials [7], [8], [9] compromising also their aesthetic quality [1], [3], [4], [5], [6], [10], [11], [12]. Biological growth on building surfaces may depend on several factors such as environment (mainly an appropriate combination of humidity, warmth, light [7], [12], [13], [14], [15]) and bioreceptivity i.e., the aptitude of a material to be colonised by living organisms [16], [17], [18]. Usually, the visual nuisance caused by deterioration and soiling is considered undesirable, especially in urban areas [2], [3], [4], [6], [10], [12], [19]; on the other hand, building envelopes are considered visually enhanced by cleaning [19]. Furthermore, biofilm growth is responsible for a large part of the weathering of building surfaces composed by stones and concrete [20].

Several authors considered cyanobacteria and green algae as pioneering inhabitants of outdoor surface [21], [22], [23], [24], [25], [26], [27]. Among them, green algae were the most frequent microorganisms and Chlorella is among the most frequent microorganisms encountered, after Klebsormidium (the most frequently recorded species in urban environments in Europe [28]). In addition to the obvious aesthetic damage, microalgal biofilms are able to dissolving stones, creating microscopic holes in their structure, increasing the substrate porosity that allow algal colonisation into the underlying layers of the substrate as well [29], [30], [31]. The alteration of the size and distribution of the pores in the material modifies the moisture circulation pattern and the response to temperature increasing its degradation process [32], [33]. Moreover, biofilms can indirectly deteriorate the colonized stone through the wide volume changes during the drying and rewetting cycles that lead to fragmentation and loss of rock fragments [12], [32], [34], [35].

Biodeterioration of external architectural surfaces may be limited by several methods, including correct design to avoid water run-off [5], the use of building materials with low bioreceptivity and the application of several treatments to hamper biological proliferation, such as water repellent products to reduce the availability of water for colonizing microorganisms and biocides to limit their biological activity [36], [37], [38], [39]. However, mainly because of leaching, traditional biocidal products may be ineffective in the long term and eventually release hazardous materials in the environment [13], [37], [40], [41], [42].

Nanoscience proved to be an alternative as well as unique resource in several fields including construction industry. Nanotechnological materials may show different and somehow unpredictable behaviours compared with their macroscopic counterparts, potentially being more efficient and less dangerous for the environment as well as more compatible with traditional materials causing limited or absent alterations of their original features [43], [44], [45], [46]. Photocatalytic materials are among the most promising tools provided by nanotechnology. Photocatalysis is the acceleration of redox mechanisms triggered by light in the presence of a catalyst [45], [47], [48], [49], [50]. This process is potentially able to degrade stains [51], [52], [53], [54], [55], [56], [57], [58], low-level pollutants [51], [56], [59], [60], [61], [62], [63], [64], [65], [66], [67], [68] and aggressive microorganisms [69], [70], [71], [72], [73], [74], [75], [76], [77] effectively limiting biological growth.

Titanium dioxide (TiO_2) in its nanometric form is a photocatalyst activated by ultraviolet (UV) light and it is the most used photocatalytic material by far especially in building industry [45], [48], [49], [78]. The biocidal effect of photostimulated nano-TiO_2 has been proved [69], [70], [71], [72], [73], [74], [75], [76], [77] but it is still under investigation. Metallic and non-metallic nanoparticles can be used to enhance nano-TiO_2 properties, such as phase stability [79], [80], [81], photoactivity [79], [80], [82] and reactivity to visible as well as UV light [79], [80], [83], [84], [85]; moreover, metals and metallic nanoparticles may show their own biocidal action [86], [87] consequently increasing the efficiency of nano-TiO_2 against biodeterioration. In addition to photocatalysis, TiO_2 nanoparticles used as surface treatment may activate a superhydrophilic phaenomenon under UV irradiation [47], [88], [89], [90], [91] that allows the formation of a thin water film on treated substrates accelerating the evaporation [92]: this process may reduce the availability of water and impede the biological growth. Several studies

already analysed the use of TiO2 to contrast algal growth on several building materials such as concrete, bricks, mortars, roof tiles [37], [39], [92], [93], [94], [95], [96], [97], [98]. More recently, TiO2 nanoparticles have been successfully used in the field of Cultural Heritage to preserve the aesthetic of several surfaces including building stones [44], [95], [99], [100], [101], [102], [103], [104], [105], [106], [107], [108], [109], [110] but the potential use of its biocidal ability on stones has been still poorly investigated.

In this work, we evaluated and compared the biocidal effectiveness of different TiO2 nanometric compounds also in combination with metallic nanoparticles – silver (Ag) and copper (Cu) – to preventively preserve the visual quality of stone surfaces from biofouling due to algal growth. Travertine, a porous calcareous natural stone, has been chosen as the reference substrate because of its high bioreceptivity and its widespread use in both historical and contemporary buildings (e.g., monuments and artworks). The aim of this study was to investigate the biodeterioration effect of a microalgal mixture composed by the green algae Chlorella sp. and Klebsormidium sp. and the cyanobacteria Phormidium sp. (Oscillatoriales) and Chlorogloeopsis sp. (Nostocales) isolated from urban architectural materials in order to investigate the performances of biocidal coatings against real algal biofilms [39]. These algae were chosen among the other isolated organisms for their ability to develop rapidly and ease to homogenise in liquid culture, allowing the easy moisten of the tested samples of travertine. Moreover, these algae are reported in other study on the bioreceptivity of various substrata [18], [37], [38], [111], [112] as well as in the ASTM D 5589–97 [113]. A laboratory test was designed to simulate the accelerated growth of algae by means of water run-off under solar including UV-A irradiation during a 9 weeks long period. In order to evaluate the influence of photocatalytic treatments on the bioreceptivity of travertine over time, we used two different complementary parameters: the extent of the area covered by algae measured through digital image analysis and the density of algal development estimated by colourimetry and spectrophotometry.

2. Materials and methods

2.1. Materials and treatment

Five different titanium dioxide aqueous solutions (sols) were prepared via sol-gel method: pure nanometric TiO2 solution (TiO2 amount: 1 wt%), two sols with both TiO2 and Ag nanoparticles (additional Ag content: 1 mol% (0.6 wt%) and 5 mol% (3.15 wt%), two sols containing both TiO2 and Cu nanoparticles (additional Cu content: 1 wt% and 5 wt%). Designations of treatments are reported in Table 1; the values of wt% are relative to the entire weight of the sol. Silver and copper were selected because of their ability to increase photoactivity of TiO2 exposed to UV light and their sterilising property [43], [49], [79], [83], [114], [115], [116], [117].

Light-coloured travertine was cut to obtain prismatic specimens (dimensions: 8.0 × 8.0 × 1.5 cm3). Three specimens were used per case study, including the untreated reference. Before treatment, all specimens were cleaned by water flow and air brushing and then dried in a ventilated oven at 103 °C until reaching the constant mass, defined as a difference between two successive daily weights less than 0.1% of the mass of specimen previously measured. The porosity of three additional travertine samples was evaluated by mercury intrusion porosimetry (Micromeritics Autopore III) according to ASTM D4404–10 [118]: an average total porosity of 5.90% was measured.

TiO2-based sols were manually sprayed on a single surface per stone specimen, in three overlapping layers per sample (gravity feed air paint spray gun, nozzle: 1.5 mm, air pressure: 6–8 bar, spraying distance: about 30 cm, product amount used per layer: 1.8 ml). Spray-coating was selected mainly because of its simplicity and feasibility of use for surface-engineered applications on monumental surfaces and architectural façades. The amount of sol applied on

stones was assessed by weighing (RADWAG Analytical XA 60/220 electronic balance, Alliance Analytical) just after the deposition of the layers: average chemical retentions of treated specimens per nanoproduct are listed in Table 1. After spray-coating, treated stones were dried in a ventilated oven at 70 °C for one hour to accelerate the drying phase (this additional drying process is not necessary in real-case application because it simply accelerates the natural drying of the coating exposed to outdoor air).

Morphology and chemical composition of stone surfaces were analysed via scanning electron microscopy. In order to have detailed information of the elemental composition of the travertine surfaces in relation to their morphology, a FEI Quanta 200 FEG Environmental Scanning Electron Microscope (FEI, Hillsboro, Oregon, USA), equipped with an energy dispersive X-ray spectrometer (EDAX inc., Mahwah, NJ, USA) was utilised.

Stone samples were deposited onto the aluminium specimen stubs previously covered with a conductive carbon adhesive disk (TAAB Ltd, Berks, England). The analysis were performed by using a strong accelerated and focalised electron beam in a vacuum (5.0 e−6 mbar), utilizing the SEM in low vacuum mode, with a chamber pressure set from 0.60 to 0.94 mbar and accelerating voltages from 10 to 20 kV. The images were obtained by means of a secondary electron detector, or with a back-scattered electron detector, with a magnification of 1000×.

The spectrometer unit was equipped with ECON (Edax Carbon Oxigen Nitrogen) 6 utw x-ray detector and a Genesis Analysis software. Each analysis was achieved with a time count of 100 s and an Amp Time of 51, while the probe current was about 290 µA.

2.2. Aesthetic compatibility

The aesthetic compatibility with treated substrates is a key prerequisite for the application of coatings on pre-existing building surfaces, especially for the preservation of Architectural Heritage. The colour of surfaces was monitored before and after treatment in order to estimate possible incompatibilities with travertine capable of deteriorate the visual quality of treated surfaces. Colourimetric measurements were carried out by means of a portable spectrophotometer (Konica Minolta CM 2000 D, diameter of circular measuring area: 3 mm) set up according to CIE standards (daylight illuminant: D65, observer angle: 10°). The results were expressed in the CIELAB colour space defined by chromatic coordinates L*, a* and b* (defining the intensity of colours in the black-white, green-magenta and blue-yellow range respectively) [119]. Colour variations after treatment were calculated according to:
(1)

where L*t, a*t and b*t and L*or, a*or and b*or are respectively the original and the post-treatment average CIELAB coordinates per specimen. Chromatic variation of each specimen was calculated considering the average of nine measurement points randomly selected per surface before and after treatment (measurements taken in triplicate for each point). Then colour changes ΔE* referred to each treatment were obtained as the average of the colour differences of three specimens per case.

2.3. Algal isolation and cultivation

The city center of Ancona (Italy) was surveyed for the presence of algal biofilms on various surfaces (buildings, soil, barks etc.). Samples were collected by scraping a surface of few cm2 with a scalpel [120] into 50-ml flasks filled with Bold's Basal Medium (BBM [121]). Several species of cyanobacteria and green algae were identified and isolated using the capillary pipette method [122] from the suspension of each flask after shaking. After an initial growth in microplates, a batch culture of single strain of Chlorella sp. (green algae), Klebsormidium sp. (green algae), Phormidium sp. (Oscillatoriales, cyanobacteria) and Chlorogloeopsis sp.

(Nostocales, cyanobacteria) was grown at 21 ± 0.1 °C under a 12:12 h L:D photoperiod and an irradiance of 90–100 mmol m−2 s−1, in 1l-flasks filled with BBM.

2.4. Accelerated algal growth test set-up

In favourable growth conditions, natural algal covering requires year to become visible and 2 up to 5 years to intensely cover architectural surfaces [123]. To accelerate algal growth on stone surfaces, a water run-off apparatus was set, similarly to previous studies [37], [38], [39], [92], [93], [123], [124], [125]; the apparatus is described in Fig. 1.

The system consisted of a glass tank (dimensions: 145 × 50 × 50 cm3) containing aluminium racks with tilted supports (45°) where no outside natural light could penetrate. The glass tank was filled with 60 L of BBM inoculated with a mixture of the four algae Chlorella sp., Klebsormidium sp., Phormidium sp. and Chlorogloeopsis sp. at final concentration of 0.5, 3.7, 3.0 and 3.0 mg/L, respectively and stones samples were placed on inclined supports without direct contact with culture medium. The microalgal mixture suspended in the culture medium was inoculated directly on moist stone surfaces through drip irrigation thus allowing the microalgal strains to flow on the sample surfaces, eventually adhering and forming a biofilm. Dripping system contained in the glass tank was constituted by a sprinkling rail made of a suspended PVC tube and a set of dripping units aligned on sample surfaces (three drippers per specimen) at a distance of about 10 mm connected to a submerged water pump (Aquarium Systems Newa Maxi-Jet, volume rate of water flow: 1000 L/h).

The apparatus was equipped with visible daylight (Philips Aqua Sky 36 W) and UV-A lamps (Wood's lamp: Philips TL-D 36/08 Blacklight Bulb, power: 36 W, wavelength range: 350–400 nm irradiance value on stone surfaces: 4.18 ± 0.56 W/m2) in order to stimulate respectively algal growth on stone substrates and photocatalysis by nanocoatings. The intensity of UV-A light on stone surfaces was quite low compared to possible peaks of natural daylight but sufficient to activate the photocatalysis of TiO2 [49], [91], [114] with no influence the kinetics of algal colonisation, since stronger UV illumination may slow down or temporarily inhibit algal growth [39], [126], [127].

Algal growth was stimulated by a cyclic day/night regime: the photoperiod, including UV illumination, was divided into 14 h day and 10 h night. Run-off cycle started simultaneously with day periods, divided into alternate on/off intervals lasting 15 min up to a total duration of 6 h (3 h on and 3 h off) with a water flow of about 5 L/h (15 L of algal inoculation for every day/night regime). A thermo-hygrometer sensor (PCE-HT71) monitored environmental conditions inside the glass chamber at a 5 min interval: average temperature and relative humidity during day/night cycles throughout the water run-off test were 25.0 ± 3.3 °C and 97.7 ± 2.8% respectively. The accelerated growth test lasted 9 weeks, sample conditions were monitored weekly as follows.

2.5. Evaluation criteria to assess algal growth on test surfaces

Two different aspects have been monitored to assess the algal colonisation on stone surfaces and therefore the efficiency of nanocoatings against biofouling during the water run-off test: the intensity and the extent of algal growth. Quantitative data were collected on a weekly basis; colour and reflectance of surfaces were examined to determine intensity and digital image analysis was used to assess the extent of algal development on stone. Furthermore, at the end of accelerated growth test, biofouled surfaces were analysed by microscopy.

Finally, in order to avoid the influence of the moisture on the aesthetical parameters considered, samples were dried for 2 h at room temperature before any measurement.

2.5.1. Colourimetry

The colour of surfaces was monitored weekly [37], [38], [92], [123] by means of the same procedure used to establish colour changes due to the application of nanomaterials, monitoring the same points per specimen. Colour changes due to the algal colonisation on stone were referred to surface aspect after treatment; each variation per specimen was determined as the mean of nine monitored points, then colour changes per case were calculated as the average of three specimens.

2.5.2. Spectrophotometry

The reflectance of surfaces toward visible light was measured simultaneously with colour by the same portable spectrophotometer (Konica Minolta CM 2000 D, daylight illuminant: D65, wavelength range: 360–740 nm, observer angle: 10°, considered wavelengths: 390–740 nm, nine measurement points per surface) in order to quantify the algal development over time [38], [123]. Reflectance spectra as a function of wavelength were measured with a 10 nm interval.

To relate the algal development to spectral reflectance curves, we considered the maximum absorption peaks of the most important pigments typically present in the selected algae: chlorophyll a and β-carotene for green algae (Chlorella sp. and Klebsormidium sp.), chlorophyll a, β-carotene and phycobilins for cyanobacteria (Phormidium sp. and Chlorogloeopsis sp.) [128]. Specific wavelengths were monitored as the absorbance peaks of the pigments: 500 nm for β-carotene and phycobilins, 630 nm for phycobilins, 680 nm for chlorophyll a.

The intensity of algal covering was quantified weekly as the average reflectance changes at specified wavelengths due to the mentioned pigments, normalizing the results with reference to original (OR) values (i.e. before the beginning of accelerated growth test) according to:
(2)

with Rn,OR and Rn,w being respectively the percentage of light reflectance at specified n wavelength (500, 630 and 680 nm) before streaming test and at the week w of accelerated growth. Reflectance value for each specimen was calculated as the average of the nine measurement points used, the average of three specimens determined the intensity of algal growth ΔRw per analysed case. In conclusion, greater reductions in the reflectance values correspond to greater intensity of algal covering.

2.5.3. Digital image analysis

The surfaces of stone specimens were scanned before the beginning of water run-off test and during accelerated algal growth on a weekly basis (EPSON Perfection V350 PHOTO, image resolution: 600 dpi). Scanning was used to get homogeneous and constant lighting, resolution and exposure. The extent of the area occupied by algal colonisation was established via digital image analysis (DIA) [37], [38], [39], [92], [111], [123] by means of ImageJ 1.48v software. The K-means-like method was used to quantify the percentage of area colonised by algae in relation to available surface: each original image (RGB coordinates) may be parted automatically by this algorithm into a given number k of classes formed by homogeneous colour zones and converted into a greyscale image having an arbitrary grey level for each partition [39], [123]. Since the algal colonisation showed different intensities and colours, we parted each original scanned image of stone surfaces into four classes (k = 4): two corresponding to non-colonised areas (white and light grey), partially contaminated surfaces (light green) and high-intensity colonisation (dark green). To identify the classes corresponding to each level of colonisation, each processed image was visually compared with the

corresponding original picture at the end of every single DIA. The number of pixels belonging to the same grey level were counted and referred to the total area of each specimen in order to obtain the percentage ratio occupied by each class (i.e. by the same level of algal growth). Sample images are given in Fig. 2.

The combination of these quantitative parameters (colour, reflectance, area covering) ensures an objective quantification of the aesthetical alteration due to algal growth on travertine, thus avoiding human's eye subjectivity.

2.5.4. Microscopical observation of algal growth

Some subsamples of each stone were fixed with 2% glutaraldehyde and dehydrated by immersion in ethanol at increasing gradations (10, 30, 50, 70, 80, 90, 95 and 100%). After one day in absolute ethanol, the dehydrated samples were treated in a Critical Point Dryer (Polaron CPD 7501). Samples were placed on stubs, and sputtered with gold-palladium in a Sputter Coater (Polaron SC 7640) for observation under scanning electron microscope (FE-SEM, Zeiss Supra 40).

2.6. Statistical analysis

To estimate the statistical significance of results, colour changes due to spray-coating and final values of antialgal efficiency measured at the end of the test were compared by one-way Anova analysis using Assistat software. The results were grouped according to the Tukey's honest significant difference (HSD) test with a significance of differences set at P-value p = 0.05.

3. Results and discussion

3.1. Microscopical analysis of coatings

The analyses performed on SEM (Fig. 3) showed that the travertine surfaces are compositionally homogeneous and generally free of contaminants. The morphology of the surfaces is compact and smooth, occasionally affected by the presence of different size cavities, due to the nature itself of the material, in which well-formed calcium carbonate crystals can be recognized (R sample).

Treated surfaces presented rather uniform coatings, but affected by widespread cracks (nT, nTA1, nTA5, nTC1, nTC5), coarse or finer, also in relation to the morphology and the compactness of the substrate. The presence of cracks has been already observed on TiO2-based nanocoatings applied on several surfaces, especially with high concentrations of TiO2 or high amount of treatment deposited on substrate [57], [100], [129]. The surfaces of the travertine specimens revealed different cracks developed in all directions, at times abundant and wide, locally smaller, but apparently not related to the kind of treatment (only TiO2, Ag or Cu containing coatings).

EDS analyses of the coating containing only TiO2 (nT) clearly revealed the presence of titanium, as well as Ag-containing coatings (nTA1, nTA5) and Cu-containing coatings (nTC1, nTC5) in which titanium was always detectable while silver or copper could only be discerned carrying out analyses for areas (not punctual) and in correspondence of zones rich in particles. In general, while the silver nanoparticles are homogeneously distributed in coatings, copper occurs in coarser particle aggregates.

3.2. Aesthetic compatibility

The application of nanotreatments under investigation did not alter significantly the colour of stone: the results of colourimetric analysis are reported in Table 2. Chromatic changes of coated surfaces were negligible since ΔE* = 1 is conventionally considered the inferior threshold for the perception of colour differences by human eye. Furthermore, colour changes up to ΔE* = 5 are considered acceptable in the field of Cultural Heritage [100], [130], [131], so the coatings are aesthetically compatible with the use on travertine for both construction and conservative purposes. The presence of metallic additives in surface treatments could cause greater and therefore unacceptable colour variations of coated substrates [87], [132]: this effect did not occur because of the restricted dimensions of metallic nanoparticles and their limited loading in the sol compositions. Coatings containing the highest amounts of metallic nanoparticles (nTA5 and nTC5) caused the greatest chromatic variations. Anyway, chromatic changes due to different treatments were not significant according to the statistical analyses carried out as described in Section 2.6.

3.3. Biocidal efficiency

Macroscopic observation of samples pointed out the algal covering of travertine with the notable exception of stone samples treated with Ag-containing coatings, irrespective of the amount of Ag used in the sol. The evolution of the visual appearance of exemplar surfaces over time is summarised in Fig. 4.

3.3.1. Colourimetry

Algal colonisation clearly altered the aspect of stone surfaces over time; colour changes due to algal growth on travertine are reported in Fig. 5. After two weeks of accelerated test, algal covering considerably modified the aspect of travertine surfaces, already beyond the acceptable limit in the field of Cultural Heritage (ΔE*>5). Average surface colours changed more intensely in the middle part of the test (weeks 2–5), until reaching very large ΔE* values (usually higher than 30), then further chromatic variations were quite limited. In the second half of the water run-off test, nTC1 showed limited variations of ΔE* thus having the best performance at the end of the 9 weeks monitoring period.

In order to better establish the presence and intensity of algal biofilm, it is important to consider chromatic coordinates L*, a* and b* separately. All cases showed a severe decrease of the L* value, indicating a darkening of the surfaces – in accordance with the growth of biofouling over the originally white surfaces of travertine specimens; Ag-containing coatings showed a partially different behaviour with an evident change of L* during the first week followed by more restrained changes. Usually a* values decreased towards green, reflecting the development of a greenish patina over stone surfaces, with the notable exception of Ag-treated surfaces during the first two weeks of the test. Furthermore, in the second half of the test, a* values went back towards their original values, thus indicating a minor presence of chlorophyll and consequently of algal biomass. This algal biomass decrease could be explained as a natural decline of algal populations, which start to die after a period of intense proliferation. The trend of b* over time was less homogeneous; anyway, the significant increase of b* value especially in the first half of the accelerated growth indicates a chromatic shift towards blue probably due to phycobilin pigments; in the second part of the test, b* variations were less pronounced, except for Ag-treated surfaces that showed a slower kinetic of colour change in the blue-yellow axis.

The colourimetric outcome of Ag-containing coatings was different from the other cases and related not only to algal contamination. Colour changes were more consistent during the first two weeks of the test than those in the other treatments, then ΔE* progression clearly

changed and remained quite constant until the end of the test; final values were similar to the other cases. Visual observation by naked eye did not notice a corresponding intense algal growth on Ag-treated surfaces; conversely they appeared almost entirely free from biological stains during the first weeks of the test. Furthermore, while colour variations were more limited after 5 weeks, nTA1 and nTA5 showed a more uniform and slower trend through the entire test without evident changes in the last weeks of the test. The most remarkable difference was in the trend of a* parameter: during the first two weeks of water run-off test, a* values shifted towards red while – as expected due to the increasing presence of chlorophyll during algal development – biofouled surfaces changed their colour towards green.

In fact, colour changes measured on Ag-treated surfaces were mostly due to a darkening effect of the coatings themselves rather than algal covering; this behaviour was confirmed by DIA analysis later reported since the area occupied by biofouling was smaller for nTA1 and nTA5. Chromatic changes can be related to the migration and consequent aggregation of silver particles on treated surfaces caused by high-humidity environment already observed in previous studies [133], [134].

In conclusion, Ag-based nanotreatments showed the minor colour changes due to algal growth and consequently the best biocidal performances, but the darkening effect due to moisture altered the aspect of treated surfaces making Ag-based nanotreatments unsuitable for the preservation of Architectural Heritage.

3.3.2. Spectrophotometry

The analysis of spectral reflectance over time clearly agreed with colourimetric results, confirming that colour changes were mostly due to the presence of algal pigments over stone surfaces corresponding to selected wavelengths. Fig. 6 shows average ΔR values during water run-off test. The variation of reflectance over time was more similar to the evolution of ΔE* values rather than that of single chromatic coordinates since the combination of different to obtain ΔR values corresponded to the monitoring of different colours over time.

Untreated surfaces showed the highest change of reflectance; nT and nTC5 had a very similar behaviour both in progression and values. In the same way as for colour changes, Ag-containing treatments showed a different trend with an evident reflectance change in the first week of the test (corresponding to the darkening effect due to the aggregation of silver nanoparticles already described) followed by a slower development in comparison with other cases. Results at the end of the experiment were slightly better than those of the majority of the other treatments, but especially before week 5 differences were clearly more evident. The behaviour of nTC1 was less homogeneous over time, especially in the second part of the water run-off test and, as already observed for colour variations, in the last week of the test there was an evident change in ΔR leading to the best performance measured at the end of the experiment.

Results of this study highlighted that higher amount of metallic nanoparticles in addition to photocatalytic TiO2 did not necessary lead to better biocidal performances.

3.3.3. Digital image analysis

Biofouling on travertine surfaces during the water run-off test was evident; Fig. 7 shows the percentage area occupied by algal biofilm.

In most cases, the surface available below the arrangement of the dripping units (about 70%) was completely and homogeneously covered by algae; photocatalytic nanotreatments usually did not inhibit (or slow down) algal growth over stone surfaces, with the significant exception of Ag-containing coatings. Differences between untreated surfaces and nT, nTC1 and nTC5 coatings were negligible and maximum algal covering was reached already after 5 weeks of

accelerated test. After reaching its maximum, the percentage area occupied by biofouling remained almost constant until the end of the 9-weeks long test.

On the other hand, Ag nanoparticles in synergy with photocatalytic TiO2 showed better biocidal performances: the progression of algal growth was slowed down noticeably and the area occupied by biofouling at the end of the test was 25% less than that of the reference case. The performance of nTA1 and nTA5 were almost the same, with significant differences in the first two weeks of the test when only nTA5 totally inhibited algal development and in the last two weeks in which a partial acceleration of algal colonisation took place on nTA5 surfaces; results at the end of the test of Ag-based coatings were basically the same. These results confirm that higher colour changes of nTA1 and nTA5 surfaces in the first part of the test were not related to algal covering but they were mostly due to the aggregation of silver nanoparticles.

The amount of metallic nanoparticles used in addition to nano-TiO2 influenced moderately the performance of the coatings: the highest content of Ag enhanced the biocidal activity only partially while no differences were noted between Cu-based treatments.

The results of DIA are consistent with the outcomes of colourimetry and spectrophotometry, with the only significant difference of nTC1 that limited the intensity of algal development without reduce its extent.

3.3.4. Microscopical observation of algal growth

SEM analysis showed a copious covering of algae on all tested stone surfaces. Although all the four algae were detected on all the samples, the cyanobacterium Phormidium sp. dominated and produced an intricate matrix in which other algal species were sporadically observed (Fig. 8). A treatment-specific effect on the community structure was not observed and the relative proportion of algal species present in the tank water was maintained on the stone surfaces. Travertine porosity strongly enhanced the algal colonisation as in that portion of stones not covered by a thick algal layer, pores were strongly colonized anyway (Fig. 8d and 8e).

The only remarkable difference among all samples observed by SEM was that the multilayer covering of algae was thicker in the untreated reference than in all other treated samples (Fig. 8b).

3.3.5. Statistical analysis

Differences between the results obtained after 9 weeks usually were not statistically relevant. Only the final values of algal covering showed some significant differences: reference stone and surfaces treated with solely TiO2 belonged to the same statistical group, Cu-containing coatings had an intermediate behaviour, while the performances of both nTA1 and nTA5 treatments were completely separated from the results of untreated surfaces, thus showing a different and better behaviour. Statistical groups for DIA analysis are reported in Fig. 7.

4. Conclusions

In this study, we analysed the inhibitory effect of photocatalytic nanocoatings against algal development on travertine surfaces in accelerated growth conditions.

The results pointed out that:

- Nanocoatings did not alter the original aspect of travertine. The majority of colour

changes measured after treatment were compatible even with their use in the preservation of Cultural Heritage, except for Ag-based treatments as visible aggregation of silver nanoparticles caused by environmental conditions during accelerated test strongly altered the original colour;
- The algal growth was only partially inhibited by nanocoatings in both intensity and extent; the most relevant performances were established by the coatings containing silver or low-percentage copper;
- The use of metallic nanoadditives in conjunction with TiO2 to increase the biocidal activity was crucial since silver and copper reduced (or slowed down) algal colonisation (anyway the algal inhibition was not directly proportional to the amount of the metallic nanoadditives); analogous studies showed similar outcomes, especially in comparison with water repellent products applied in order to reduce bioreceptivity [37], [39].

Further investigations performed in order to better establish the biocidal efficiency of photocatalytic nanotreatments against algal development on architectural stone surfaces related to several parameters are strongly recommended.

In this regards, other factors should be considered for the future investigations:
- more intense UV illumination (compatible with natural daylight values) could increase photoactivity and therefore the biocidal performances of TiO2-based nanocoatings with limited or temporary alteration to the vitality of algae [39], so further investigation on the effect of UV light intensity on photoactivity of TiO2 against algal growth are recommended;
- the acceleration due to the environmental conditions and the set-up of water run-off test could be too high and consequently inappropriate for the identification of the anti-algal properties of the photocatalytic surface in real case application;
- dead algae may create a barrier effect leading to (i) reduce the contact between living algal cells deposited by dripping and underlying reactive oxygen species created by nanocoatings and (ii) limit the amount of UV light received by photocatalytic nanoparticles and therefore their activity;
- the vigour and adherence of algal biofilm still attached to stone surfaces at the end of the accelerated growth should be assessed in order to establish its resistance to possible further cleaning actions (as for example washing).

Acknowledgements

The authors would like to thank Professor Pietro Gobbi of University of Urbino and Dr Claudio Pizzagalli of ARPAM Department, Pesaro, for having kindly provided the necessary equipment for microscopic analyses. The nanotech company Salentec srl (Lecce, Italy) is highly acknowledged for the kind support of the nanocompounds used in this study.

References

[1]
P.J. Creighton, P.J. Lioy, F.H. Haynie, T.J. Lemmons, J.L. Miller, J. Gerhart
Soiling by atmospheric aerosols in an urban industrial area
J. Air Waste Manag. Assoc., 40 (1990), pp. 1285-1289, 10.1080/10473289.1990.10466783

[2]
C.A. Pio, M.M. Ramos, A.C. Duarte
Atmospheric aerosol and soiling of external surfaces in an urban environment
Atmos. Environ., 32 (1998), pp. 1979-1989, 10.1016/S1352-2310(97)00507-4

[3]
C.M. Grossi, R.M. Esbert, F. Díaz-Pache, F.J. Alonso
Soiling of building stones in urban environments
Build. Environ., 38 (2003), pp. 147-159, 10.1016/S0360-1323(02)00017-3

[4]
C.M. Grossi, P. Brimblecombe, R.M. Esbert, F.J. Alonso
Color changes in architectural limestones from pollution and cleaning
Color Res. Appl., 32 (2007), pp. 320-331, 10.1002/col.20322

[5]
M.Y.L. Chew, P.P. Tan
Facade staining arising from design features
Constr. Build. Mater., 17 (2003), pp. 181-187

[6]
M. Urosevic, A. Yebra-Rodríguez, E. Sebastián-Pardo, C. Cardell
Black soiling of an architectural limestone during two-year term exposure to urban air in the city of Granada (S Spain)
Sci. Total Environ., 414 (2012), pp. 564-575, 10.1016/j.scitotenv.2011.11.028

[7]
C. Saiz-Jimenez
Biodeterioration vs biodegradation: the role of microorganisms in the removal of pollutants deposited on historic buildings
Int. Biodeterior. Biodegr., 40 (1997), pp. 225-232, 10.1016/S0964-8305(97)00035-8

[8]
C. Gaylarde, M. Ribas Silva, T. Warscheid
Microbial impact on building materials: an overview
Mater. Struct. Constr., 36 (2003), pp. 342-352, 10.1617/13867

[9]
N. De Belie
Microorganisms versus stony materials: a love–hate relationship
Mater. Struct., 43 (2010), pp. 1191-1202, 10.1617/s11527-010-9654-0

[10]
E.F. Doehne, C.A. Price
Stone Conservation: an Overview of Current Research
(second ed.), Getty Conservation Institute, Los Angeles (2010)

[11]
R. Kumar
Biodeterioration of Stone in Tropical Environments: an Overview
Getty Conservation Institute, Los Angeles (1999)

[12]
J.J. Ortega-Calvo, X. Ariño, M. Hernandez-Marine, C. Saiz-Jimenez
Factors affecting the weathering and colonization of monuments by phototrophic microorganisms
Sci. Total Environ., 167 (1995), pp. 329-341, 10.1016/0048-9697(95)04593-P

[13]

P. Tiano
Biodegradation of Cultural Heritage: Decay Mechanisms and Control Methods
Semin. Artic. New Univ. Lisbon Dep. Conserv. Restor.
(2002), pp. 7-12

[14]
A. Jain, S. Bhadauria, V. Kumar, R.S. Chauhan
Biodeterioration of sandstone under the influence of different humidity levels in laboratory conditions
Build. Environ., 44 (2009), pp. 1276-1284, 10.1016/j.buildenv.2008.09.019

[15]
S. Johansson, L. Wadsö, K. Sandin
Estimation of mould growth levels on rendered façades based on surface relative humidity and surface temperature measurements
Build. Environ., 45 (2010), pp. 1153-1160, 10.1016/j.buildenv.2009.10.022

[16]
O. Guillitte
Bioreceptivity: a new concept for building ecology studies
Sci. Total Environ., 167 (1995), pp. 215-220, 10.1016/0048-9697(95)04582-L

[17]
C.C. Gaylarde, P.M. Gaylarde
A comparative study of the major microbial biomass of biofilms on exteriors of buildings in Europe and Latin America
Int. Biodeterior. Biodegr., 55 (2005), pp. 131-139, 10.1016/j.ibiod.2004.10.001

[18]
A.Z. Miller, P. Sanmartín, L. Pereira-Pardo, A. Dionísio, C. Saiz-Jimenez, M.F. Macedo, B. Prieto
Bioreceptivity of building stones: a review
Sci. Total Environ., 426 (2012), pp. 1-12, 10.1016/j.scitotenv.2012.03.026

[19]
P. Brimblecombe, C.M. Grossi
Aesthetic thresholds and blackening of stone buildings
Sci. Total Environ., 349 (2005), pp. 175-189, 10.1016/j.scitotenv.2005.01.009

[20]
B. De Graef, V. Cnudde, J. Dick, N. De Belie, P. Jacobs, W. Verstraete
A sensitivity study for the visualisation of bacterial weathering of concrete and stone with computerised X-ray microtomography
Sci. Total Environ., 341 (2005), pp. 173-183, 10.1016/j.scitotenv.2004.09.035

[21]
J.J. Ortega-Calvo, M. Hernandez-Marine, C. Saiz-Jimenez
Biodeterioration of building materials by cyanobacteria and algae
Int. Biodeterior., 28 (1991), pp. 165-185, 10.1016/0265-3036(91)90041-O

[22]
P. Tiano, P. Accolla, L. Tomaselli
Phototrophic biodeteriogens on lithoid surfaces: an ecological study
Microb. Ecol., 29 (1995), pp. 299-309, 10.1007/BF00164892

[23]

G. Cecchi, L. Pantani, V. Raimondi, L. Tomaselli, G. Lamenti, P. Tiano, R. Chiari
Fluorescence lidar technique for the remote sensing of stone monuments
J. Cult. Herit., 1 (2000), pp. 29-36

[24]
G. Lamenti, P. Tiano, L. Tomaselli
Biodeterioration of ornamental marble statues in the boboli gardens (Florence, Italy)
J. Appl. Phycol., 12 (2000), pp. 427-433

[25]
L. Tomaselli, P. Tiano, G. Lamenti
Occurrence and fluctuation in photosynthetic biocoenoses dwelling on stone monuments
O. Ciferri, P. Tiano, G. Mastromei (Eds.), Microbes Art, Springer, US (2000), pp. 63-76

[26]
C.A. Crispim, C.C. Gaylarde
Cyanobacteria and biodeterioration of cultural heritage: a review
Microb. Ecol., 49 (2005), pp. 1-9, 10.1007/s00248-003-1052-5

[27]
M.F. Macedo, A.Z. Miller, A. Dionisio, C. Saiz-Jimenez
Biodiversity of cyanobacteria and green algae on monuments in the mediterranean basin: an overview
Microbiology, 155 (2009), pp. 3476-3490, 10.1099/mic.0.032508-0

[28]
F. Rindi
Diversity, distribution and ecology of green algae and cyanobacteria in urban habitats
D.J. Seckbach (Ed.), Algae Cyanobacteria Extreme Environ, Springer, Netherlands (2007), pp. 619-638

[29]
P.S. Griffin, N. Indictor, R.J. Koestler
The biodeterioration of stone: a review of deterioration mechanisms, conservation case histories, and treatment
Int. Biodeterior., 28 (1991), pp. 187-207

[30]
P. Fernandes
Applied microbiology and biotechnology in the conservation of stone cultural heritage materials
Appl. Microbiol. Biotechnol., 73 (2006), pp. 291-296, 10.1007/s00253-006-0599-8

[31]
P. Gaylarde, G. Englert, O. Ortega-Morales, C. Gaylarde
Lichen-like colonies of pure Trentepohlia on limestone monuments
Int. Biodeterior. Biodegr., 58 (2006), pp. 119-123, 10.1016/j.ibiod.2006.05.005

[32]
C. Saiz-Jimenez
Biogeochemistry of weathering processes in monuments
Geomicrobiol. J., 16 (1999), pp. 27-37, 10.1080/014904599270721

[33]
T. Warscheid, J. Braams

Biodeterioration of stone: a review
Int. Biodeterior. Biodegr., 46 (2000), pp. 343-368, 10.1016/S0964-8305(00)00109-8

[34]
M.E. Young, H.-L. Alakomi, I. Fortune, A.A. Gorbushina, W.E. Krumbein, I. Maxwell, C. McCullagh, P. Robertson, M. Saarela, J. Valero, M. Vendrell
Development of a biocidal treatment regime to inhibit biological growths on cultural heritage: BIODAM
Environ. Geol., 56 (2008), pp. 631-641, 10.1007/s00254-008-1455-1

[35]
A. Kemmling, M. Kämper, C. Flies, O. Schieweck, M. Hoppert
Biofilms and extracellular matrices on geomaterials
Environ. Geol., 46 (2004), 10.1007/s00254-004-1044-x

[36]
C. Urzì, F. De Leo
Evaluation of the efficiency of water-repellent and biocide compounds against microbial colonization of mortars
Int. Biodeterior. Biodegr., 60 (2007), pp. 25-34, 10.1016/j.ibiod.2006.11.003

[37]
A. Maury-Ramirez, W. De Muynck, R. Stevens, K. Demeestere, N. De Belie
Titanium dioxide based strategies to prevent algal fouling on cementitious materials
Cem. Concr. Compos, 36 (2013), pp. 93-100, 10.1016/j.cemconcomp.2012.08.030

[38]
W. De Muynck, A. Maury-Ramirez, N. De Belie, W. Verstraete
Evaluation of strategies to prevent algal fouling on white architectural and cellular concrete
Int. Biodeterior. Biodegr., 63 (2009), pp. 679-689, 10.1016/j.ibiod.2009.04.007

[39]
T. Martinez, A. Bertron, G. Escadeillas, E. Ringot
Algal growth inhibition on cement mortar: efficiency of water repellent and photocatalytic treatments under UV/VIS illumination
Int. Biodeterior. Biodegr., 89 (2014), pp. 115-125, 10.1016/j.ibiod.2014.01.018

[40]
F. Chen, X. Yang, Q. Wu
Antifungal capability of TiO2 coated film on moist wood
Build. Environ., 44 (2009), pp. 1088-1093, 10.1016/j.buildenv.2008.07.018

[41]
A. Unger
Decontamination and “deconsolidation” of historical wood preservatives and wood consolidants in cultural heritage
J. Cult. Herit., 13 (2012), pp. S196-S202, 10.1016/j.culher.2012.01.015

[42]
M. Shabir Mahr, T. Hübert, I. Stephan, H. Militz
Decay protection of wood against brown-rot fungi by titanium alkoxide impregnations
Int. Biodeterior. Biodegr., 77 (2013), pp. 56-62, 10.1016/j.ibiod.2012.04.026

[43]
S.N. Kartal, F. Green, C.A. Clausen

Do the unique properties of nanometals affect leachability or efficacy against fungi and termites?
Int. Biodeterior. Biodegr., 63 (2009), pp. 490-495, 10.1016/j.ibiod.2009.01.007

[44]
P. Baglioni, E. Carretti, D. Chelazzi
Nanomaterials in art conservation
Nat. Nanotechnol., 10 (2015), pp. 287-290

[45]
F. Pacheco-Torgal, S. Jalali
Nanotechnology: advantages and drawbacks in the field of construction and building materials
Constr. Build. Mater., 25 (2011), pp. 582-590, 10.1016/j.conbuildmat.2010.07.009

[46]
M. Brai, L. Tranchina, M. Alberghina, D. Fontana, F. Fernandez (Eds.), Diagnostics for Cultural Heritage: Analytical Approach for an Effective Conservation, Università degli Studi di Palermo, Palermo (2014)
Diagn. Cult. Herit. Anal. Approach Eff. Conserv.

[47]
A. Fujishima, X. Zhang, D. Tryk
TiO2 photocatalysis and related surface phenomena
Surf. Sci. Rep., 63 (2008), pp. 515-582, 10.1016/j.surfrep.2008.10.001

[48]
J. Chen, C. Poon
Photocatalytic construction and building materials: from fundamentals to applications
Build. Environ., 44 (2009), pp. 1899-1906, 10.1016/j.buildenv.2009.01.002

[49]
S. Guo, Z. Wu, W. Zhao
TiO2-based building materials: above and beyond traditional applications
Chin. Sci. Bull., 54 (2009), pp. 1137-1142, 10.1007/s11434-009-0063-0

[50]
K. Nakata, A. Fujishima
TiO2 photocatalysis: design and applications
J. Photochem. Photobiol. C Photochem. Rev., 13 (2012), pp. 169-189, 10.1016/j.jphotochemrev.2012.06.001

[51]
J. Chen, S. Kou, C. Poon
Photocatalytic cement-based materials: comparison of nitrogen oxides and toluene removal potentials and evaluation of self-cleaning performance
Build. Environ., 46 (2011), pp. 1827-1833, 10.1016/j.buildenv.2011.03.004

[52]
X. Zhao, Q. Zhao, J. Yu, B. Liu
Development of multifunctional photoactive self-cleaning glasses
J. Non-Cryst. Solids, 354 (2008), pp. 1424-1430, 10.1016/j.jnoncrysol.2006.10.093

[53]
B. Ruot, A. Plassais, F. Olive, L. Guillot, L. Bonafous
TiO2-containing cement pastes and mortars: measurements of the photocatalytic efficiency

using a rhodamine B-based colourimetric test
Sol. Energy, 83 (2009), pp. 1794-1801, 10.1016/j.solener.2009.05.017

[54]
S. de Niederhãusern, M. Bondi, F. Bondioli
Self-cleaning and antibacteric ceramic tile surface
Int. J. Appl. Ceram. Technol., 10 (2013), pp. 949-956, 10.1111/j.1744-7402.2012.02801.x

[55]
F. Bondioli, R. Taurino, A.M. Ferrari
Functionalization of ceramic tile surface by sol–gel technique
J. Colloid Interface Sci., 334 (2009), pp. 195-201, 10.1016/j.jcis.2009.02.054

[56]
E. Quagliarini, F. Bondioli, G.B. Goffredo, C. Cordoni, P. Munafò
Self-cleaning and de-polluting stone surfaces: TiO2 nanoparticles for limestone
Constr. Build. Mater., 37 (2012), pp. 51-57, 10.1016/j.conbuildmat.2012.07.006

[57]
P. Munafò, E. Quagliarini, G.B. Goffredo, F. Bondioli, A. Licciulli
Durability of nano-engineered TiO2 self-cleaning treatments on limestone
Constr. Build. Mater., 65 (2014), pp. 218-231, 10.1016/j.conbuildmat.2014.04.112

[58]
M.-Z. Guo, A. Maury-Ramirez, C.S. Poon
Self-cleaning ability of titanium dioxide clear paint coated architectural mortar and its potential in field application
J. Clean. Prod., 112 (2016), pp. 3583-3588, 10.1016/j.jclepro.2015.10.079

[59]
N.S. Allen, M. Edge, J. Verran, J. Stratton, J. Maltby, C. Bygott
Photocatalytic titania based surfaces: environmental benefits
Polym. Degrad. Stab., 93 (2008), pp. 1632-1646, 10.1016/j.polymdegradstab.2008.04.015

[60]
J. Mo, Y. Zhang, Q. Xu, J.J. Lamson, R. Zhao
Photocatalytic purification of volatile organic compounds in indoor air: a literature review
Atmos. Environ., 43 (2009), pp. 2229-2246, 10.1016/j.atmosenv.2009.01.034

[61]
T. Maggos, J.G. Bartzis, M. Liakou, C. Gobin
Photocatalytic degradation of NOx gases using TiO2-containing paint: a real scale study
J. Hazard. Mater., 146 (2007), pp. 668-673, 10.1016/j.jhazmat.2007.04.079

[62]
T. Maggos, J.G. Bartzis, P. Leva, D. Kotzias
Application of photocatalytic technology for NOx removal
Appl. Phys. A, 89 (2007), pp. 81-84, 10.1007/s00339-007-4033-6

[63]
G. Hüsken, M. Hunger, H.J.H. Brouwers
Experimental study of photocatalytic concrete products for air purification
Build. Environ., 44 (2009), pp. 2463-2474, 10.1016/j.buildenv.2009.04.010

[64]

R. de_Richter, S. Caillol
Fighting global warming: the potential of photocatalysis against CO2, CH4, N2O, CFCs, tropospheric O3, BC and other major contributors to climate change
J. Photochem. Photobiol. C Photochem. Rev., 12 (2011), pp. 1-19, 10.1016/j.jphotochemrev.2011.05.002

[65]
A. Maury-Ramirez, K. Demeestere, N. De Belie
Photocatalytic activity of titanium dioxide nanoparticle coatings applied on autoclaved aerated concrete: effect of weathering on coating physical characteristics and gaseous toluene removal
J. Hazard. Mater., 211–212 (2012), pp. 218-225, 10.1016/j.jhazmat.2011.12.037

[66]
M.-Z. Guo, C.-S. Poon
Photocatalytic NO removal of concrete surface layers intermixed with TiO2
Build. Environ., 70 (2013), pp. 102-109, 10.1016/j.buildenv.2013.08.017

[67]
A. Maury-Ramirez, J.-P. Nikkanen, M. Honkanen, K. Demeestere, E. Levänen, N. De Belie
TiO2 coatings synthesized by liquid flame spray and low temperature sol–gel technologies on autoclaved aerated concrete for air-purifying purposes
Mater. Charact., 87 (2014), pp. 74-85, 10.1016/j.matchar.2013.10.025

[68]
J. Hot, T. Martinez, B. Wayser, E. Ringot, A. Bertron
Photocatalytic degradation of NO/NO2 gas injected into a 10-m3 experimental chamber
Environ. Sci. Pollut. Res. (2016), 10.1007/s11356-016-7701-2

[69]
O.K. Dalrymple, E. Stefanakos, M.A. Trotz, D. Yogi Goswami
A review of the mechanisms and modeling of photocatalytic disinfection
Appl. Catal. B Environ., 98 (2010), pp. 27-38, 10.1016/j.apcatb.2010.05.001

[70]
T. Matsunaga, M. Okochi
TiO2-mediated photochemical disinfection of Escherichia coli using optical fibers
Environ. Sci. Technol., 29 (1995), pp. 501-505, 10.1021/es00002a028

[71]
K. Sunada, Y. Kikuchi, K. Hashimoto, A. Fujishima
Bactericidal and detoxification effects of TiO2 thin film photocatalysts
Environ. Sci. Technol., 32 (1998), pp. 726-728

[72]
P.-C. Maness, S. Smolinski, D.M. Blake, Z. Huang, E.J. Wolfrum, W.A. Jacoby
Bactericidal activity of photocatalytic TiO2 reaction: toward an understanding of its killing mechanism
Appl. Environ. Microbiol., 65 (1999), pp. 4094-4098

[73]
M. Cho, H. Chung, W. Choi, J. Yoon
Linear correlation between inactivation of E. coli and OH radical concentration in TiO2 photocatalytic disinfection
Water Res., 38 (2004), pp. 1069-1077, 10.1016/j.watres.2003.10.029

[74]
O. Seven, B. Dindar, S. Aydemir, D. Metin, M. Ozinel, S. Icli
Solar photocatalytic disinfection of a group of bacteria and fungi aqueous suspensions with TiO2, ZnO and Sahara desert dust
J. Photochem. Photobiol. Chem., 165 (2004), pp. 103-107, 10.1016/j.jphotochem.2004.03.005

[75]
C. Sichel, J. Tello, M. de Cara, P. Fernández-Ibáñez
Effect of UV solar intensity and dose on the photocatalytic disinfection of bacteria and fungi
Catal. Today, 129 (2007), pp. 152-160, 10.1016/j.cattod.2007.06.061

[76]
J. Hong, H. Ma, M. Otaki
Controlling algal growth in photo-dependent decolorant sludge by photocatalysis
J. Biosci. Bioeng., 99 (2005), pp. 592-597, 10.1263/jbb.99.592

[77]
J.R. Peller, R.L. Whitman, S. Griffith, P. Harris, C. Peller, J. Scalzitti
TiO2 as a photocatalyst for control of the aquatic invasive alga, Cladophora, under natural and artificial light
J. Photochem. Photobiol. Chem., 186 (2007), pp. 212-217, 10.1016/j.jphotochem.2006.08.009

[78]
W. Zhu, P.J.M. Bartos, A. Porro
Application of nanotechnology in construction
Mater. Struct., 37 (2004), pp. 649-658, 10.1617/14234

[79]
J.M. Coronado, F. Fresno, M.D. Hernández-Alonso, R. Portela (Eds.), Design of Advanced Photocatalytic Materials for Energy and Environmental Applications, Springer London, London (2013)

[80]
L.G. Devi, R. Kavitha
A review on non metal ion doped titania for the photocatalytic degradation of organic pollutants under UV/solar light: role of photogenerated charge carrier dynamics in enhancing the activity
Appl. Catal. B Environ., 140–141 (2013), pp. 559-587, 10.1016/j.apcatb.2013.04.035

[81]
D.A.H. Hanaor, M.H.N. Assadi, S. Li, A. Yu, C.C. Sorrell
Ab initio study of phase stability in doped TiO2
Comput. Mech., 50 (2012), pp. 185-194, 10.1007/s00466-012-0728-4

[82]
Y.C. Lee, Y.P. Hong, H.Y. Lee, H. Kim, Y.J. Jung, K.H. Ko, H.S. Jung, K.S. Hong
Photocatalysis and hydrophilicity of doped TiO2 thin films
J. Colloid Interface Sci., 267 (2003), pp. 127-131, 10.1016/S0021-9797(03)00603-9

[83]
M. Pelaez, N.T. Nolan, S.C. Pillai, M.K. Seery, P. Falaras, A.G. Kontos, P.S.M. Dunlop, J.W.J. Hamilton, J.A. Byrne, K. O'Shea, M.H. Entezari, D.D. Dionysiou
A review on the visible light active titanium dioxide photocatalysts for environmental applications
Appl. Catal. B Environ., 125 (2012), pp. 331-349, 10.1016/j.apcatb.2012.05.036

[84]
J. Chen, F. Qiu, W. Xu, S. Cao, H. Zhu
Recent progress in enhancing photocatalytic efficiency of TiO2-based materials
Appl. Catal. Gen., 495 (2015), pp. 131-140, 10.1016/j.apcata.2015.02.013

[85]
M. Asiltürk, F. Sayılkan, E. Arpaç
Effect of Fe3+ ion doping to TiO2 on the photocatalytic degradation of Malachite Green dye under UV and vis-irradiation
J. Photochem. Photobiol. Chem., 203 (2009), pp. 64-71, 10.1016/j.jphotochem.2008.12.021

[86]
M. Aflori, B. Simionescu, I.-E. Bordianu, L. Sacarescu, C.-D. Varganici, F. Doroftei, A. Nicolescu, M. Olaru
Silsesquioxane-based hybrid nanocomposites with methacrylate units containing titania and/or silver nanoparticles as antibacterial/antifungal coatings for monumental stones
Mater. Sci. Eng. B, 178 (2013), pp. 1339-1346, 10.1016/j.mseb.2013.04.004

[87]
S.A. Ruffolo, A. Macchia, M.F. La Russa, L. Mazza, C. Urzì, F. De Leo, M. Barberio, G.M. Crisci
Marine antifouling for underwater archaeological sites: TiO2 and Ag-doped TiO2
Int. J. Photoenergy, 2013 (2013), pp. 1-6, 10.1155/2013/251647

[88]
A. Fujishima, T.N. Rao, D.A. Tryk
Titanium dioxide photocatalysis
J. Photochem. Photobiol. C Photochem. Rev., 1 (2000), pp. 1-21, 10.1016/S1389-5567(00)00002-2

[89]
A. Fujishima, X. Zhang
Titanium dioxide photocatalysis: present situation and future approaches
Comptes Rendus Chim., 9 (2006), pp. 750-760, 10.1016/j.crci.2005.02.055

[90]
R. Wang, K. Hashimoto, A. Fujishima, M. Chikuni, E. Kojima, A. Kitamura, M. Shimohigoshi, T. Watanabe
Light-induced amphiphilic surfaces
Nature, 388 (1997), pp. 431-432, 10.1038/41233

[91]
A. Fujishima, T.N. Rao, D. Tryk
TiO2 photocatalysts and diamond electrodes
Electrochim. Acta, 45 (2000), pp. 4683-4690, 10.1016/S0013-4686(00)00620-4

[92]
Z. Zhang, J. MacMullen, H.N. Dhakal, J. Radulovic, C. Herodotou, M. Totomis, N. Bennett
Biofouling resistance of titanium dioxide and zinc oxide nanoparticulate silane/siloxane exterior facade treatments
Build. Environ., 59 (2013), pp. 47-55, 10.1016/j.buildenv.2012.08.006

[93]
K. Gröplová, K. Čabanová, P. Bábková, M. Vaculík, V. Matějka, J. Kukutschová, Pavla Čapková
Testing the Effects Biodeteriorations Green Algae Chlorella Vulgaris on Samples with

Photoactive Composites Kaoline/TiO2
Getty Conservation Institute, Los Angeles (1999)

[94]
C.A. Linkous, G.J. Carter, D.B. Locuson, A.J. Ouellette, D.K. Slattery, L.A. Smitha
Photocatalytic inhibition of algae growth using TiO2, WO3, and cocatalyst modifications
Environ. Sci. Technol., 34 (2000), pp. 4754-4758, 10.1021/es001080+

[95]
A.J. Fonseca, F. Pina, M.F. Macedo, N. Leal, A. Romanowska-Deskins, L. Laiz, A. Gómez-Bolea, C. Saiz-Jimenez
Anatase as an alternative application for preventing biodeterioration of mortars: evaluation and comparison with other biocides
Int. Biodeterior. Biodegr., 64 (2010), pp. 388-396, 10.1016/j.ibiod.2010.04.006

[96]
F. Gladis, R. Schumann
Influence of material properties and photocatalysis on phototrophic growth in multi-year roof weathering
Int. Biodeterior. Biodegr., 65 (2011), pp. 36-44, 10.1016/j.ibiod.2010.05.014

[97]
M.-Z. Guo, A. Maury-Ramirez, C.S. Poon
Versatile photocatalytic functions of self-compacting architectural glass mortars and their inter-relationship
Mater. Des., 88 (2015), pp. 1260-1268, 10.1016/j.matdes.2015.09.133

[98]
M.-Z. Guo, A. Maury-Ramirez, C.S. Poon
Photocatalytic activities of titanium dioxide incorporated architectural mortars: effects of weathering and activation light
Build. Environ., 94 (2015), pp. 395-402, 10.1016/j.buildenv.2015.08.027

[99]
P. Munafò, G.B. Goffredo, E. Quagliarini
TiO2-based nanocoatings for preserving architectural stone surfaces: an overview
Constr. Build. Mater., 84 (2015), pp. 201-218, 10.1016/j.conbuildmat.2015.02.083

[100]
E. Franzoni, A. Fregni, R. Gabrielli, G. Graziani, E. Sassoni
Compatibility of photocatalytic TiO2-based finishing for renders in architectural restoration: a preliminary study
Build. Environ, 80 (2014), pp. 125-135, 10.1016/j.buildenv.2014.05.027

[101]
M.F. La Russa, S.A. Ruffolo, N. Rovella, C.M. Belfiore, A.M. Palermo, M.T. Guzzi, G.M. Crisci
Multifunctional TiO2 coatings for cultural heritage
Prog. Org. Coat., 74 (2012), pp. 186-191, 10.1016/j.porgcoat.2011.12.008

[102]
F. Gherardi, A. Colombo, M. D'Arienzo, B. Di Credico, S. Goidanich, F. Morazzoni, R. Simonutti, L. Toniolo
Efficient self-cleaning treatments for built heritage based on highly photo-active and well-dispersible TiO2 nanocrystals
Microchem. J., 126 (2016), pp. 54-62, 10.1016/j.microc.2015.11.043

[103]
L. Bergamonti, F. Bondioli, I. Alfieri, A. Lorenzi, M. Mattarozzi, G. Predieri, P.P. Lottici
Photocatalytic self-cleaning TiO2 coatings on carbonatic stones
Appl. Phys. A, 122 (2016), 10.1007/s00339-015-9560-y

[104]
F. Pino, P. Fermo, M. La Russa, S. Ruffolo, V. Comite, J. Baghdachi, E. Pecchioni, F. Fratini, G. Cappelletti
Advanced mortar coatings for cultural heritage protection. Durability towards prolonged UV and outdoor exposure
Environ. Sci. Pollut. Res. (2016), 10.1007/s11356-016-7611-3

[105]
M. Lettieri, A. Calia, A. Licciulli, A.E. Marquardt, R.J. Phaneuf
Nanostructured TiO2 for stone coating: assessing compatibility with basic stone's properties and photocatalytic effectiveness
Bull. Eng. Geol. Environ. (2015), 10.1007/s10064-015-0820-z

[106]
A. Calia, M. Lettieri, M. Masieri
Durability assessment of nanostructured TiO2 coatings applied on limestones to enhance building surface with self-cleaning ability
Build. Environ., 110 (2016), pp. 1-10, 10.1016/j.buildenv.2016.09.030

[107]
L. Bergamonti, I. Alfieri, A. Lorenzi, G. Predieri, G. Barone, G. Gemelli, P. Mazzoleni, S. Raneri, D. Bersani, P.P. Lottici
Nanocrystalline TiO2 coatings by sol–gel: photocatalytic activity on Pietra di Noto biocalcarenite
J. Sol-Gel Sci. Technol. (2015), 10.1007/s10971-015-3684-6

[108]
L. Bergamonti, I. Alfieri, A. Lorenzi, A. Montenero, G. Predieri, R. Di Maggio, F. Girardi, L. Lazzarini, P.P. Lottici
Characterization and photocatalytic activity of TiO2 by sol–gel in acid and basic environments
J. Sol-Gel Sci. Technol., 73 (2015), pp. 91-102, 10.1007/s10971-014-3498-y

[109]
A. Colombo, F. Gherardi, S. Goidanich, J.K. Delaney, E.R. de la Rie, M.C. Ubaldi, L. Toniolo, R. Simonutti
Highly transparent poly(2-ethyl-2-oxazoline)-TiO 2 nanocomposite coatings for the conservation of matte painted artworks
RSC Adv., 5 (2015), pp. 84879-84888, 10.1039/C5RA10895K

[110]
C. Beccaria, A. Colombo, F. Gherardi, V. Mombrini, L. Toniolo
Use of nanocoatings for the restoration of matte paintings
Stud. Conserv., 61 (2016), pp. 265-266, 10.1080/00393630.2016.1183958

[111]
H. Barberousse, B. Ruot, C. Yéprémian, G. Boulon
An assessment of façade coatings against colonisation by aerial algae and cyanobacteria
Build. Environ., 42 (2007), pp. 2555-2561, 10.1016/j.buildenv.2006.07.031

[112]
G. Escadeillas, A. Bertron, P. Blanc, A. Dubosc
Accelerated testing of biological stain growth on external concrete walls. Part 1: development of the growth tests
Mater. Struct., 40 (2007), pp. 1061-1071, 10.1617/s11527-006-9205-x

[113]
ASTM International
ASTM D 5589 Standard Test Method for Determining the Resistance of Paint Films and Related Coatings to Algal Defacement
(1997)

[114]
K. Hashimoto, H. Irie, A. Fujishima
TiO2 photocatalysis: a historical overview and future prospects
Jpn. J. Appl. Phys., 44 (2005), p. 8269, 10.1143/JJAP.44.8269

[115]
G. Mantanis, E. Terzi, S.N. Kartal, A.N. Papadopoulos
Evaluation of mold, decay and termite resistance of pine wood treated with zinc- and copper-based nanocompounds
Int. Biodeterior. Biodegr., 90 (2014), pp. 140-144, 10.1016/j.ibiod.2014.02.010

[116]
D.B. Hamal, J.A. Haggstrom, G.L. Marchin, M.A. Ikenberry, K. Hohn, K.J. Klabunde
A multifunctional biocide/sporocide and photocatalyst based on titanium dioxide (TiO2) codoped with silver, carbon, and sulfur
Langmuir, 26 (2010), pp. 2805-2810, 10.1021/la902844r

[117]
L. Pinho, M. Rojas, M.J. Mosquera
Ag–SiO2–TiO2 nanocomposite coatings with enhanced photoactivity for self-cleaning application on building materials
Appl. Catal. B Environ., 178 (2015), pp. 144-154, 10.1016/j.apcatb.2014.10.002

[118]
ASTM International
ASTM D 4404 Standard Test Method for Determination of Pore Volume and Pore Volume Distribution of Soil and Rock by Mercury Intrusion Porosimetry
(2010)

[119]
UNI Ente Nazionale Italiano di Unificazione
UNI EN 15886 Conservation of Cultural Property Test Methods Colour Measurement of Surfaces
(2010)

[120]
F. Rindi, M.D. Guiry
Diversity, life history, and ecology of Trentepohlia and Printzina (Trentepohliales, chlorophyta) in urban habitats in Western Ireland
J. Phycol., 38 (2002), pp. 39-54, 10.1046/j.1529-8817.2002.01193.x

[121]
H.W. Bischoff, H.C. Bold

Some Soil Algae from Enchanted Rock and Related Algal Species
University of Texas, Austin, Tex (1963)

[122]
R.W. Hoshaw, J.R. Rosowski
Methods for microscopic algae
J.R. Stein (Ed.), Handb. Phycol. Methods Cult. Methods Growth Meas, Cambridge University Press, New York (1973), pp. 53-67

[123]
G. Escadeillas, A. Bertron, E. Ringot, P.J. Blanc, A. Dubosc
Accelerated testing of biological stain growth on external concrete walls. Part 2: quantification of growths
Mater. Struct., 42 (2009), pp. 937-945, 10.1617/s11527-008-9433-3

[124]
O. Guillitte, R. Dreesen
Laboratory chamber studies and petrographical analysis as bioreceptivity assessment tools of building materials
Sci. Total Environ., 167 (1995), pp. 365-374, 10.1016/0048-9697(95)04596-S

[125]
A. Dubosc, G. Escadeillas, P.J. Blanc
Characterization of biological stains on external concrete walls and influence of concrete as underlying material
Cem. Concr. Res., 31 (2001), pp. 1613-1617, 10.1016/S0008-8846(01)00613-5

[126]
U. Karsten, S. Lembcke, R. Schumann
The effects of ultraviolet radiation on photosynthetic performance, growth and sunscreen compounds in aeroterrestrial biofilm algae isolated from building facades
Planta, 225 (2007), pp. 991-1000, 10.1007/s00425-006-0406-x

[127]
F. Gladis, R. Schumann
A suggested standardised method for testing photocatalytic inactivation of aeroterrestrial algal growth on TiO2-coated glass
Int. Biodeterior. Biodegr., 65 (2011), pp. 415-422, 10.1016/j.ibiod.2011.01.005

[128]
L.E. Graham, J.M. Graham, L.W. Wilcox, M.E. Cook
Algae
LJLM Press (2016)

[129]
A. Licciulli, A. Calia, M. Lettieri, D. Diso, M. Masieri, S. Franza, R. Amadelli, G. Casarano
Photocatalytic TiO2 coatings on limestone
J. Sol-Gel Sci. Technol., 60 (2011), pp. 437-444, 10.1007/s10971-011-2574-9

[130]
C. Miliani, M.L. Velo-Simpson, G.W. Scherer
Particle-modified consolidants: a study on the effect of particles on sol–gel properties and consolidation effectiveness
J. Cult. Herit., 8 (2007), pp. 1-6, 10.1016/j.culher.2006.10.002

[131]
O. García, K. Malaga
Definition of the procedure to determine the suitability and durability of an anti-graffiti product for application on cultural heritage porous materials
J. Cult. Herit., 13 (2012), pp. 77-82, 10.1016/j.culher.2011.07.004

[132]
L. Bergamonti, I. Alfieri, M. Franzò, A. Lorenzi, A. Montenero, G. Predieri, M. Raganato, A. Calia, L. Lazzarini, D. Bersani, P.P. Lottici
Synthesis and characterization of nanocrystalline TiO2 with application as photoactive coating on stones
Environ. Sci. Pollut. Res., 21 (2014), pp. 13264-13277, 10.1007/s11356-013-2136-5

[133]
E. Ando, M. Miyazaki
Moisture degradation mechanism of silver-based low-emissivity coatings
Thin Solid Films, 351 (1999), pp. 308-312, 10.1016/S0040-6090(98)01796-9

[134]
E. Ando, S. Suzuki, N. Aomine, M. Miyazaki, M. Tada
Sputtered silver-based low-emissivity coatings with high moisture durability
Vacuum, 59 (2000), pp. 792-799, 10.1016/S0042-207X(00)00349-3

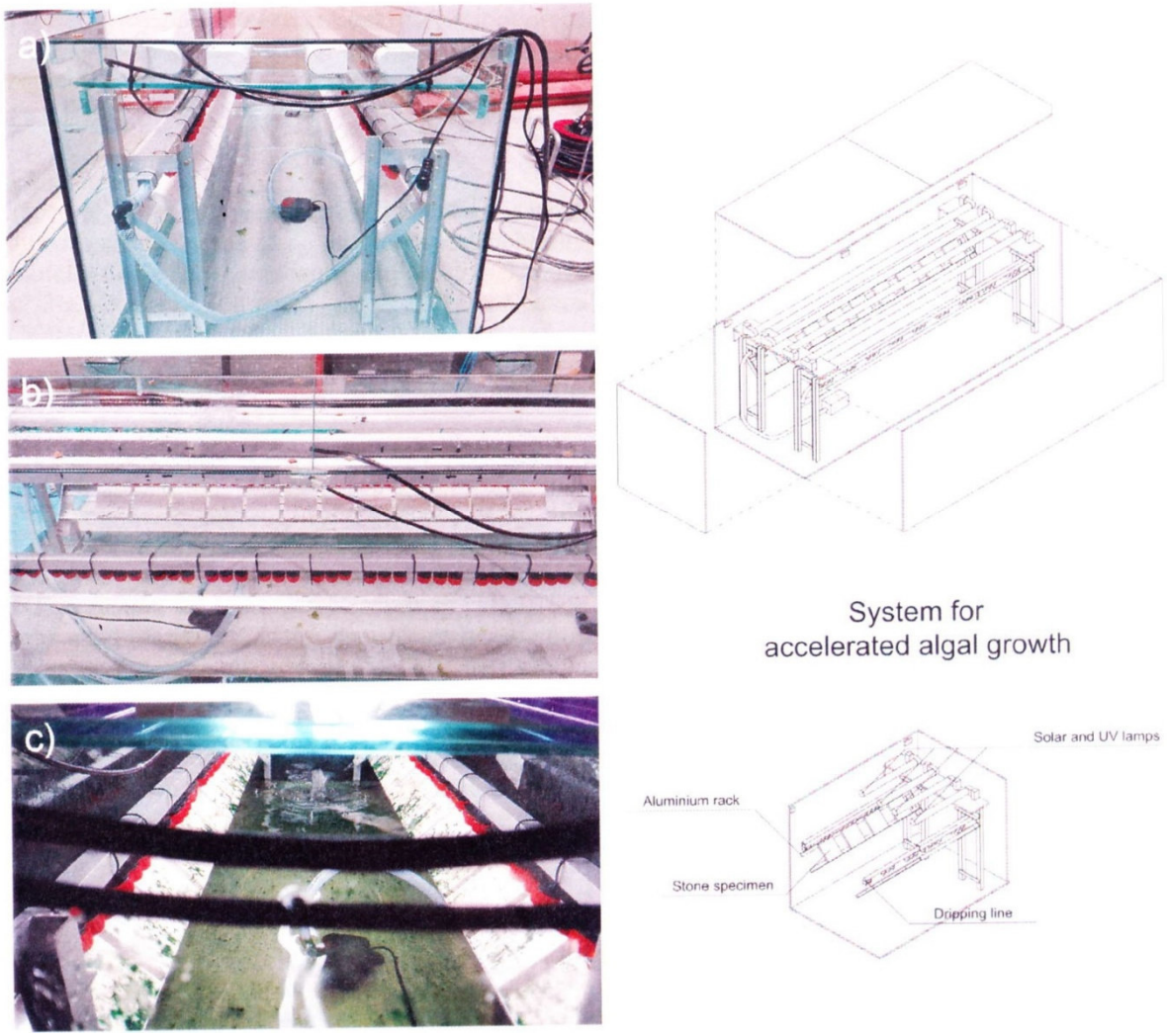

Fig. 1. DIA: K-means like method, sample partition in four classes during water run-off test. Dark and middle grey clusters identify clean surfaces. light grey are low-colonised greenish areas and high-colonised areas are made black by the algorithm.

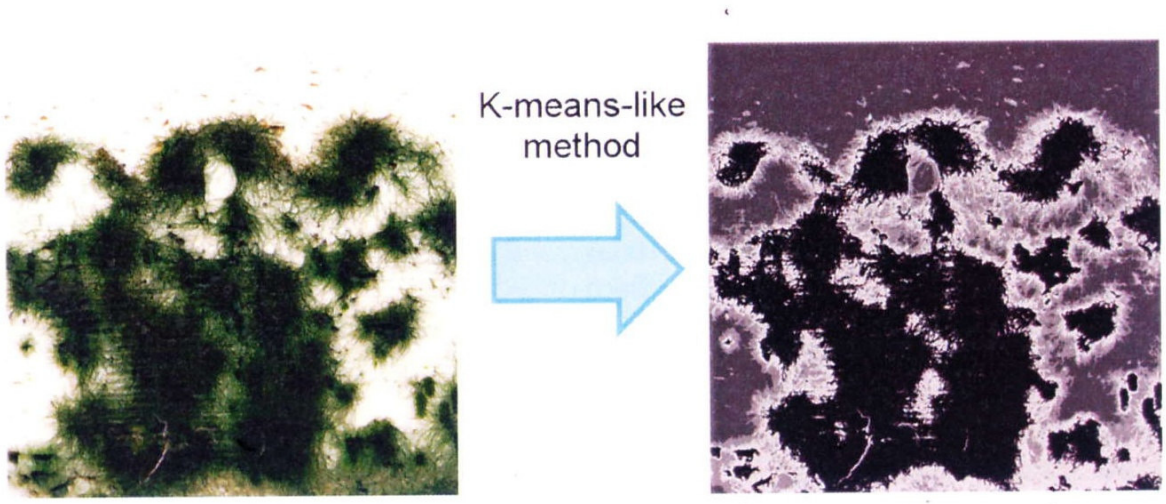

Fig. 2. System used for the accelerated algal growth test: (a) system over view, (b) detail of specimens on the racks under dnppers. (c) test chamber after 3 weeks of accelerated algal growth. The glass chamber was covered during the test to avoid any influence by external light

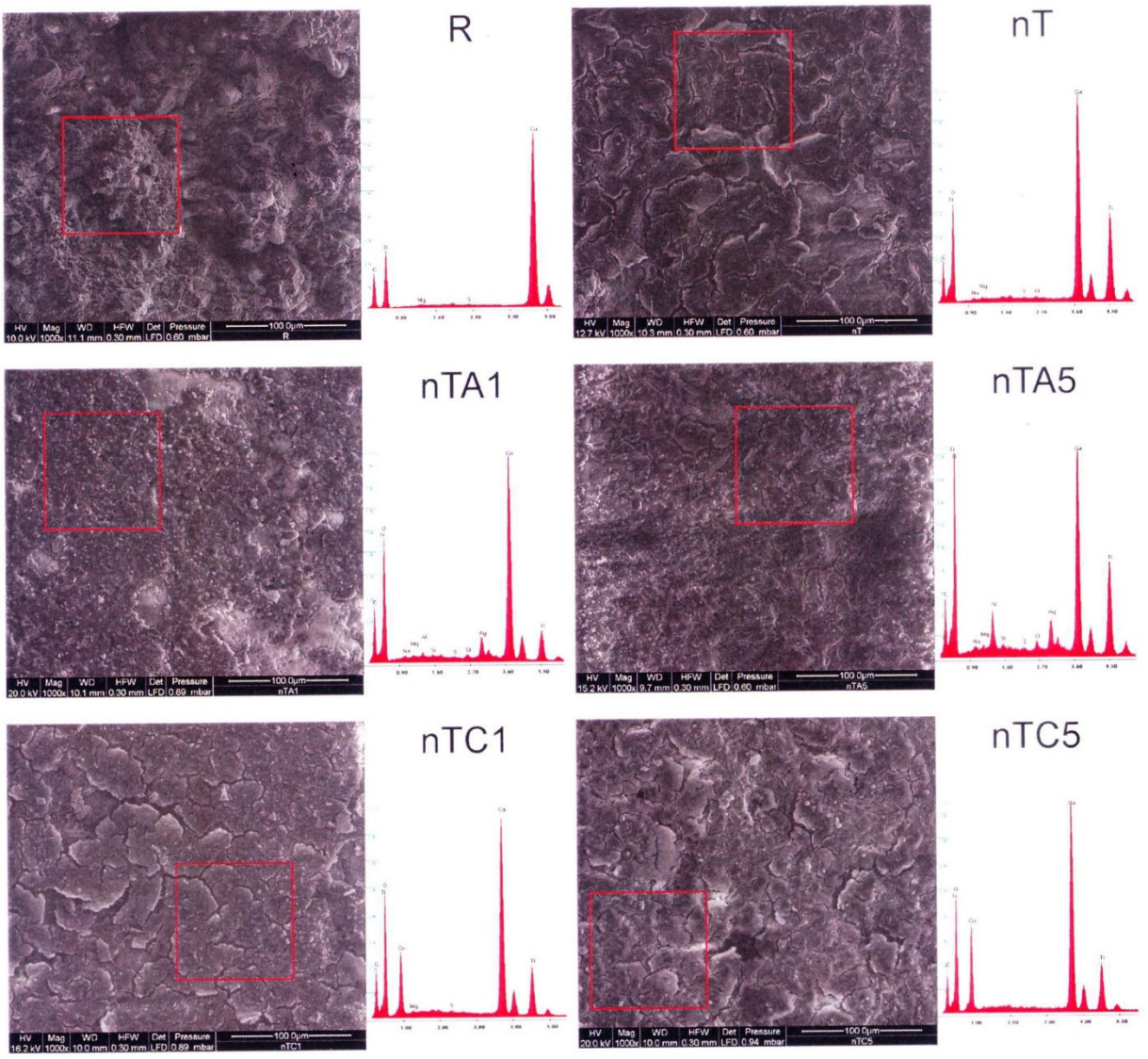

Fig. 3. Microscopic analyses of trave rt ine surfa ces befo re accelerated algal g rowth test: SEM images (magnit ude 1.000 x , detectio n area for EDS ana lyses reported as red squares) and EDS spectr,1 (to the rig ht of the correspond ing SEM images). (Fo,- interpr etat ion of the referen ces to colo ur in this figur e lege nd, the reader 1s referred to the web ve rsion of this arti cle

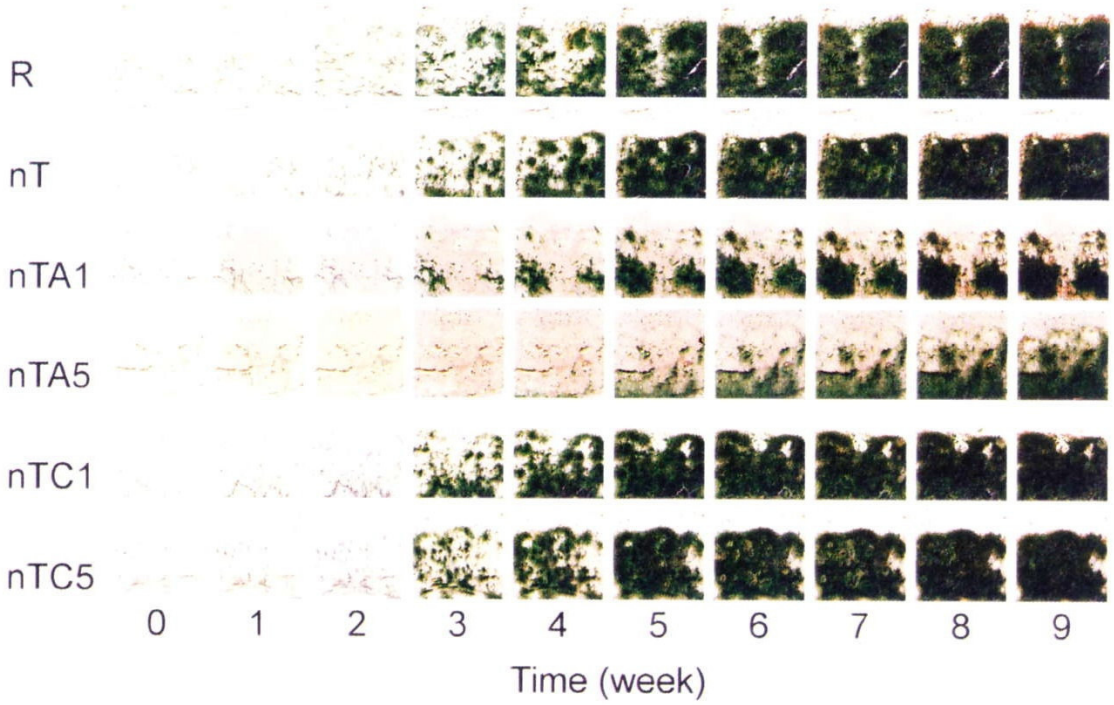

Fig. 4. Weekly progression of the macroscopic visual appearance of tested surfaces during water run-off test

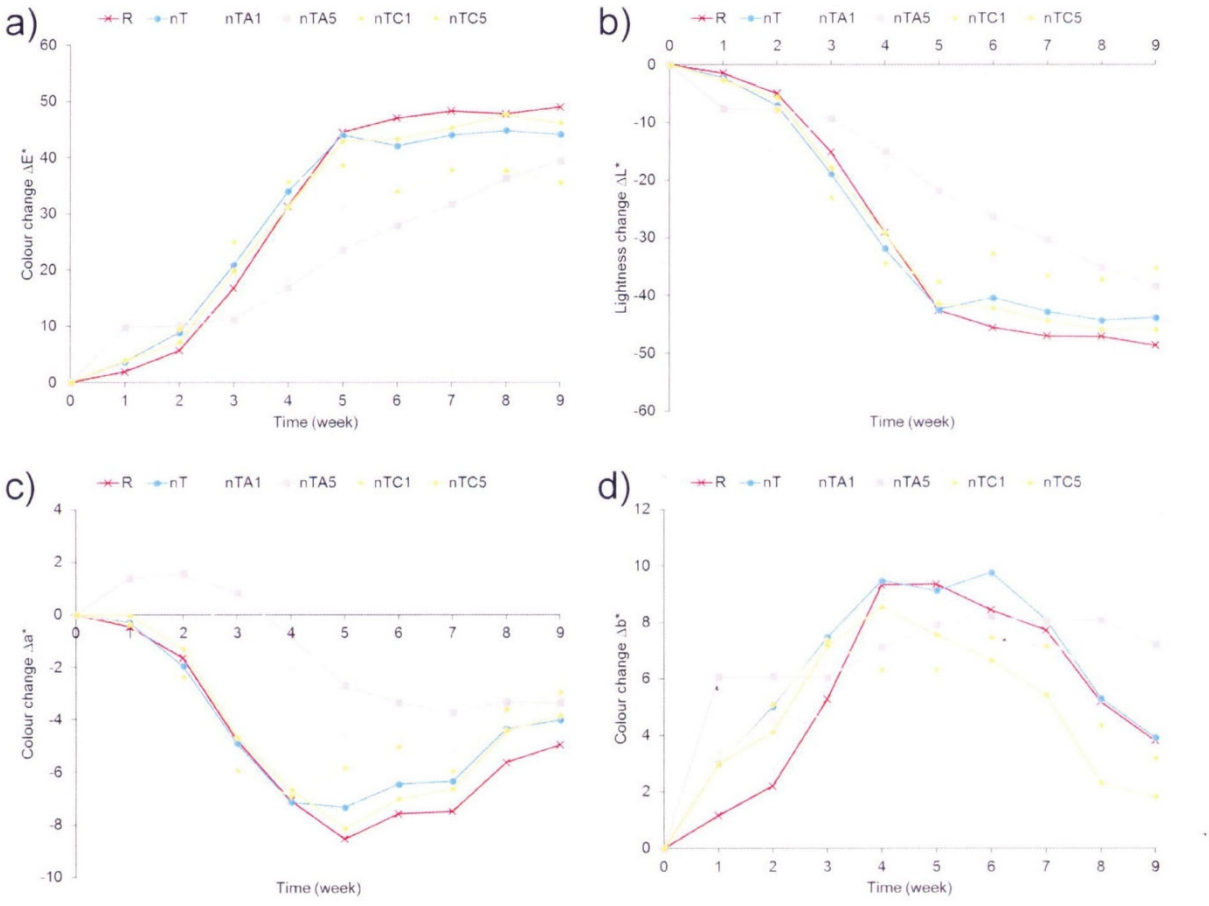

Fig. 5. Intensity of algal fouling: colour changes during water run-off test. mean values (n = 3); total colour change CIE' (a) and variations of single chromatic coordinates L', a' and b' are reported separately (b. c. d respectively

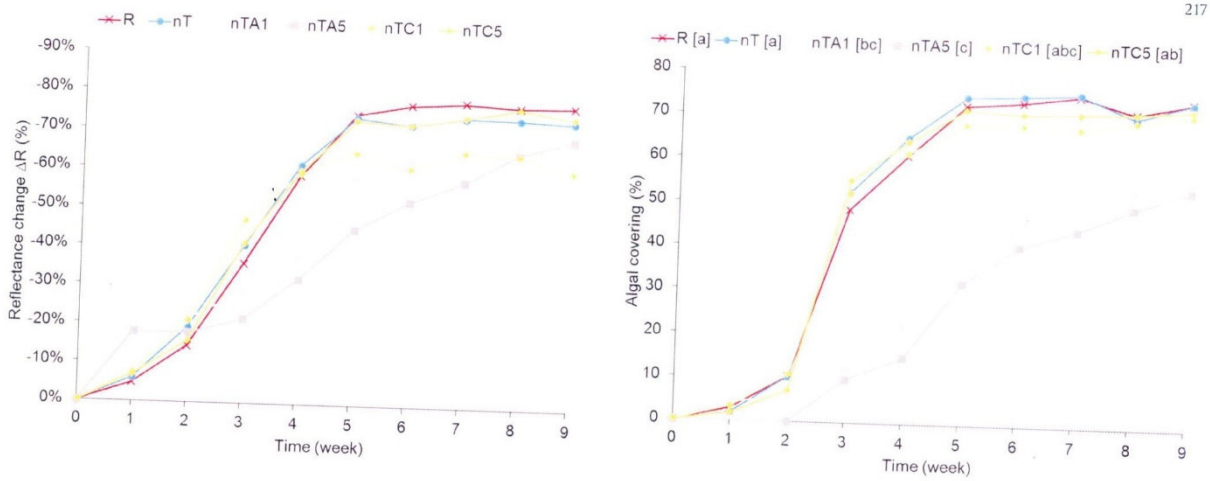

Fig. 6. I nten si ty of alg al fou li ng: ave rage ren ectance chan ges du ri ng wate r run -o ff test (n; 3) monitored by spectrophotometr

Fig. 7. Extent of the alg al fou li ng: evo lu tio n of the area covered by .ilgal co lo nis at io n dur i ng the water run -off test. mea n val ues (pe rcent age up to tota l. n; 3). Lette rs i n to square brac ke ts i nd icate the affili atio n of the outcomes at the e nd of the tes t to res pec tive s tati stic al group s; cases wi t ho ut comm o n le tters are sig nificantly diffe re n t according to HSD analy sis.

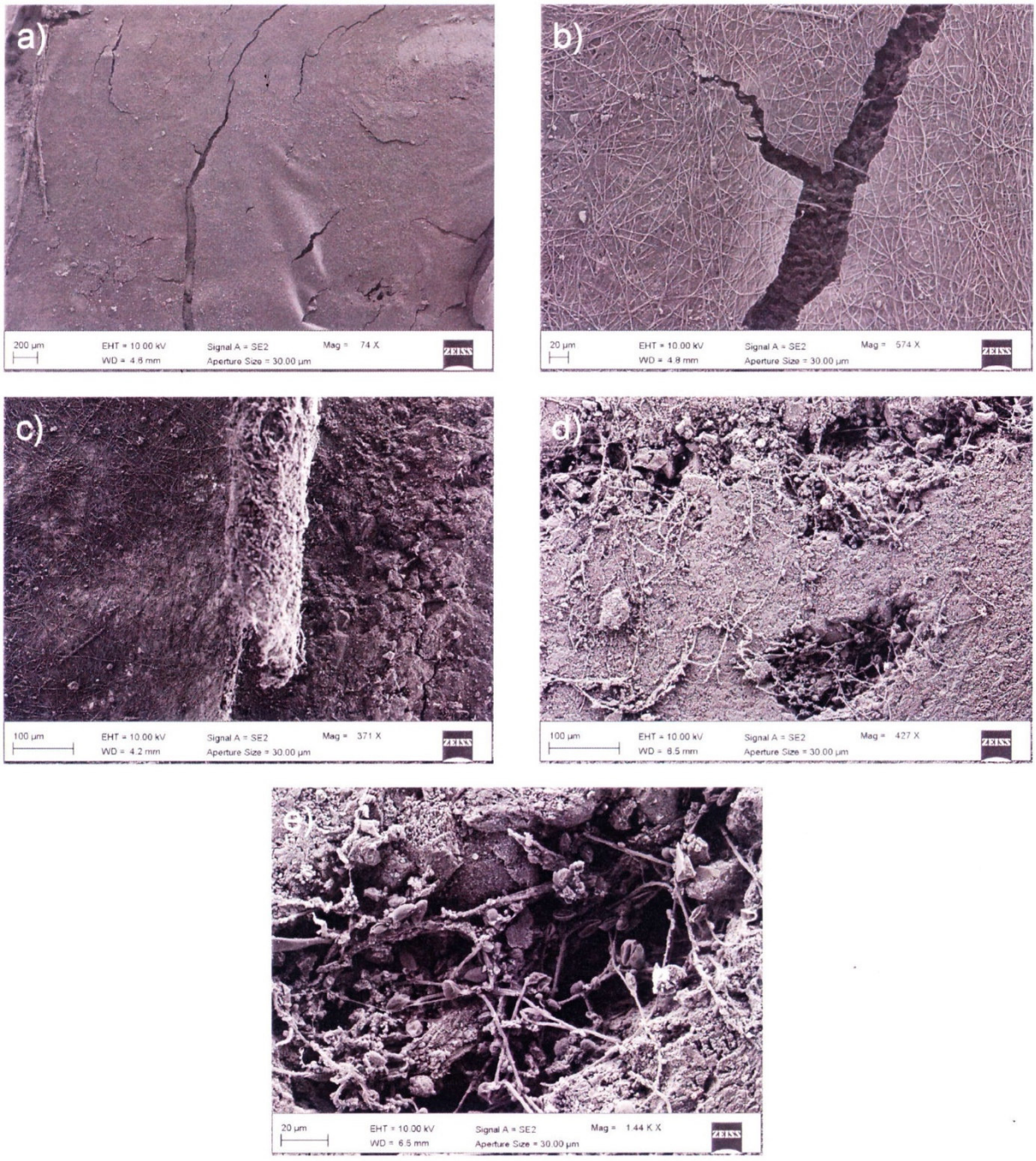

Fig. 8. Algal biofilm grown on travertine surfaces. (a, b) Untreated refer ence sho wing a wide and thick algal multila yer, with an intricate matrix of the cyanobacterium Phormid ium sp. on the cop layer (a) and cell s of the green alga Chlorella sp. visible through the fissures in the top level (b). (c- e) Treated stones nTCl. nTCS and nTCS. re sp ectively; algal biofilm leaves uncovered the right part of the stone surface (c) where algal cell s are mainly concentr ate d inside the pores of the stone (d); Chlorella sp . and Phormidium sp. do minate th e algal communit y inside the pore (e